

# Visualization of Simultaneous Changes in Multiple Motion Features with Spatial Volume and Flat Arrows for Sports Motion Analysis

Tomoya Shiokawa<sup>[0009-0006-4409-1946]</sup>, Kunio Yamamoto<sup>[0009-0000-2463-732X]</sup>,  
and Masaki Oshita<sup>[0000-0001-9844-7713]</sup>

Kyushu Institute of Technology, Fukuoka, Japan  
shiokawa.tomoya408@mail.kyutech.jp  
kunio@ai.kyutech.ac.jp  
oshita@ai.kyutech.ac.jp

**Abstract.** It is important for beginners practicing sports motions such as tennis shots or baseball batting to check their own body movements and the correct movements of skilled players, and to understand the differences between them. However, checking each change in the features of a body part in motion, such as the position, orientation, movement speed, and rotational speed, is labor intensive. In this study, we propose a method for visualizing simultaneous changes in multiple features of one body part in one input motion with the spatial volume and flat arrows. In our method, the changes in the three-dimensional (3D) position and one-dimensional (1D) movement speed of a body part are simultaneously visualized as a spatial volume along the trajectory of the body part, the radius of which varies with the movement speed. In addition, changes in the 3D orientation of the body part and 1D rotational speed are visualized using flat arrows, the size of which changes according to the rotational speed. By generating these volumes and arrows for each motion of beginners and experts, users can easily check for changes in the features of body parts during these motions. In addition, users can identify problems in their own motion by comparing these. Finally, we present experimental examples of tennis shot and baseball batting motions.

**Keywords:** Human motion · Motion feature · Visualization

## 1 Introduction

It is effective for beginners practicing sports motions such as tennis shots or baseball batting to imitate the motions of experts. To achieve this, it is necessary to understand the changes in the characteristic quantities of the position, orientation, movement speed, and rotational speed of body parts in the movements of oneself and an expert as well as the differences between them. However, checking the changes in each feature individually is labor intensive.

To solve this problem, this study proposes a method to visualize simultaneous changes in multiple features of one body part in an input motion with

the spatial volume and flat arrows. In our method, the changes in the three-dimensional (3D) position and one-dimensional (1D) movement speed of a body part are simultaneously visualized as a spatial volume along the trajectory of the body part, the radius of which varies with the movement speed. In addition, the changes in the 3D orientation of the body part and 1D rotational speed are visualized as a series of flat arrows, the size of which changes according to the rotational speed. In this case, the arrows are drawn at the point where the body part has moved or rotated by a certain amount, so that the arrows are displayed appropriately even in a range where the orientation changes rapidly. Users can review the visualized volumes or arrows of the body parts of the motion to grasp the changes in the features. They can also compare the visualization of the motions of an expert and a novice to identify problems in the motions of novices. In this study, we applied our methods to forehand shot motions in tennis and batting motions in baseball, and evaluated the visualized results to determine whether users could grasp the changes between the motions of an expert and a novice.

The remainder of this paper is organized as follows: Section 2 outlines related research and Section 3 describes the visualization system for motion features. Sections 4 and 5 describe the methods for generating the spatial volume and flat arrows, respectively. Section 6 presents the experimental results and discussion, and Section 7 concludes the paper.

## 2 Related Work

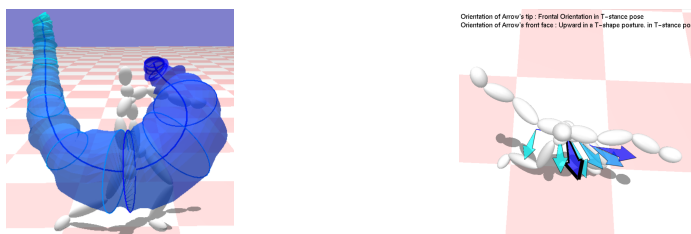
Several training systems are aimed at imitating the motions of experts [1][2][3]. However, these only display the motions of beginners and experts and do not specifically visualize the changes in the features of each motion or the differences between them.

Several techniques have been developed for evaluating motions. For example, a method has been proposed that draws motion as a single image [4] and another method draws important postures on a timeline [5]. However, obtaining information regarding movement, rotational speed, and orientation using these methods is difficult. Zhang et al. [6] developed the MoSculp system, which generates 3D shapes to represent the trajectories of body parts in motion; however, this system cannot represent information regarding orientation or speed.

Many methods are available for visualizing changes in the positions and orientations of body parts during motion. Oshita [7] proposed a method for visualizing the temporal changes in the 3D position of a body part by generating a spatial volume in which the distance from the trajectory is constant. However, this method only visualizes the change in position and cannot capture information on the movement speed of the body part. A method has also been proposed to visualize temporal changes in the 3D orientation of a body part by generating a flat arrow; however, this method only visualizes the change in orientation and does not include information on the rotational speed. In addition, this method generates arrows at constant distance intervals; if the orientation changes sig-

nificantly over a short distance, important information regarding the change in orientation is lost.

### 3 Motion Feature Visualization System



(a) Features (position and movement speed)

(b) Features (orientation and rotational speed)

Fig. 1: Example visualization of the change in features in a forehand shot of an expert. (a) Visualizing changes in body part position and movement speed with spatial volume. (b) Visualizing changes in orientation and rotational speed of body parts with the direction and size of flat arrows.

#### 3.1 Inputs and Outputs of System

The input data for this system are motion data of a novice and an expert obtained using a motion capture device, a body part, and two features. Selectable body parts are one of the major body parts (hand, foot, chest, waist, or knee); features include the position or orientation and speed of movement or rotation. Users select the body part and feature information to be visualized using keyboard operations. From this information, the system generates spatial volumes or a series of flat arrows for each input motion, which visualizes the changes in motion features. By observing them, users can review the simultaneous changes in the features that they select. They can also grasp the differences in motion between the novice and expert by reviewing or comparing the visualization results. When drawing an arrow, the correspondence between the direction of the arrow and that of the body part is displayed on the screen, as shown in Figure 1(b). The volumes and arrows are generated using translucent polygons, and those generated from each motion are distinguished by colors. In addition, the postures of the beginner and expert motions are represented by black and white stick figures, respectively.

The input motion data are represented as a series of postures  $\mathbf{P}$ . When a human body model is provided,  $\mathbf{P}$  is expressed as  $\mathbf{P} = \{\mathbf{p}, \mathbf{o}, \mathbf{r}_1, \dots, \mathbf{r}_n\}$ , where  $\mathbf{p}$  is the waist position,  $\mathbf{r}$  is the waist orientation, and  $\mathbf{r}_i$  are rotations of all joints. The position  $\mathbf{p}$  is a 3D vector, and in this study, the orientation  $\mathbf{o}$  and rotation  $\mathbf{r}$  are represented by a  $3 \times 3$  matrix. The positions and orientations of the body

parts in any frame, which are necessary to obtain the features, are computed using forward kinematics.

### 3.2 Auxiliary Functions

The system provides a function that allows the user to play, stop, and rewind the input motion, thereby enabling the user to check the motion in detail. The system also allows the user to change the position of the camera and gaze point freely, making it easier to grasp the shape of the motion, generated volumes, and arrows. Several other auxiliary functions are also provided to make it easier to grasp the appearance of changes in features when visualizing them using volumes and arrows.

Emphasizing the shape of the volume in our method makes it easier to grasp changes in the position and movement speed of body parts. Therefore, we prepared a function to display the volume shape at regular movement distance intervals using curves, as shown in Figure 1(a). This function can be activated or deactivated by keyboard operations. In this study, the movement distance interval was set to  $0.4f$ .

By checking the features during the playback of the motion, the user can grasp the changes in feature values in more detail. Therefore, this system displays the shapes of the volume and arrow, which represent the features at the playback time of the motion. The shape of the displayed volume is a curve, as shown in Figure 1(a), and the arrow has a thick outer frame, as shown in Figure 1(b). Whether this function is enabled can be toggled using keyboard operations.

Visualizing changes in the feature values for the entire section is undesirable if the acquired motions include motions that are superfluous compared with those originally intended to be confirmed. There may also be cases in which the user wishes to confirm the changes in features only in some sections. In such cases, this system provides a function that allows the user to change the visualization section freely through keyboard operations.

## 4 Spatial Volume Generation

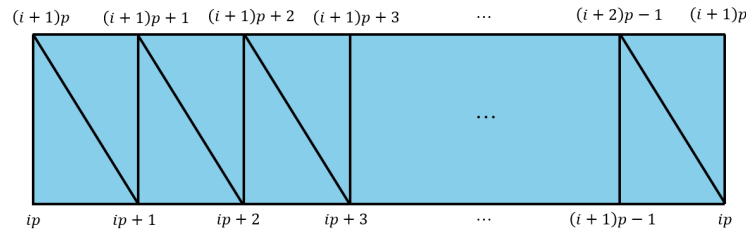


Fig. 2: Method of surface generation

This section describes our method for simultaneously visualizing the changes in position  $\mathbf{p}$  and movement speed  $v$  of one body part in the visualization section of one motion as a spatial volume along the trajectory of the body part, the radius  $r$  of which changes depending on the movement speed. The positions of the body parts in each frame of motion are computed using forward kinematics. The movement speed is calculated by dividing the distance moved in one frame by the time interval between the frames of motion. In this study, the user selects one of the major body parts (hand, foot, chest, waist, or knee), and volumes are generated for each motion at that site. To add time information, we change the color of the volume for  $\frac{1}{10}$  frames in the motion visualization section. The volume generated from the expert motion is changed from teal to blue, and that generated by the beginner motion is changed from yellow to red.

To generate a volume surface along the trajectory of the part with a radius  $r$ , it is necessary to generate a set of vertices of the surface  $\mathbf{P}$  in the range perpendicular to and  $r$  away from the trajectory. Therefore,  $\mathbf{P}$  is calculated using the radius  $r$  and two vectors  $vecu$  and  $vecv$  perpendicular to the movement vector between frames and perpendicular to each other, respectively. That is,

$$\mathbf{P} = r(\mathbf{u}\cos\theta + \mathbf{v}\sin\theta), \quad (1)$$

where the range of  $\theta$  is  $0 \leq \theta < 2\pi$ , and in this study,  $p$ , the number of point clouds  $\mathbf{P}_i$  generated from each frame, is set to 30. The radius  $r_i$  of the volume at each time point is calculated as follows:

$$r_i = r_{min} + cv_i, \quad (2)$$

where  $r_{min}$  is the base value of the radius and  $c$  is a constant for adjusting the radius. In this study, the volume is generated as  $r_{min} = 0.05f$  and  $c = 0.025f$ . A radius adjustment method is available in which the maximum and minimum changes in the radius are standardized for all parts. However, this method reduces the visibility of the generated volumes for body parts with short trajectories, such as the chest and waist; therefore, we do not use this method in this study.

Anomalous movement speeds or fine fluctuations in trajectories can cause the shape of the volume to become uneven. Therefore, we perform two pre-processing steps. Before determining the radius using Equation (2), we replace  $v_i$  that satisfies  $v_i < \frac{v_m}{2}$  or  $v_i > 2v_m$  with  $v_m$ , where  $v_m$  is the average value of the movement speed in the previous and subsequent frames. The trajectories are smoothed by averaging the positions of the three frames. To generate the surface of the volume, we do not use a surface generation method such as the marching cubes method [8]. Instead, we use a simple method in which the surface is constructed using triangular polygons with vertices specified from a point cloud. The sides of the volume are generated by specifying  $p$  points generated from the  $i$ th and  $i + 1$ th frames, as shown in Figure (2). The faces closing both ends of the volume are generated as regular  $p$ -sided polygons with vertices that are the points generated in the first and last frames.

## 5 Flat Arrow Generation

This section describes our method for simultaneously visualizing the changes in 3D orientation  $v_x, v_y, v_z$  and rotational speed  $r$  of one body part in the visualization section of one motion as flat arrows with a size that changes with the rotational speed. We also explain the setting of appropriate drawing intervals and adjustment of the number of drawings according to the viewpoint, which is performed to improve the visibility.

### 5.1 Generation of Arrows

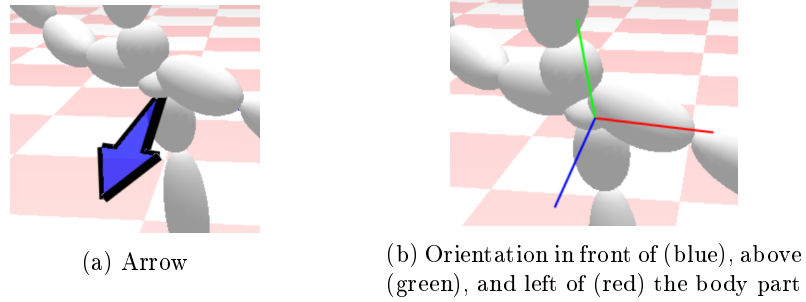


Fig. 3: Correspondence between arrows and orientation of body part.

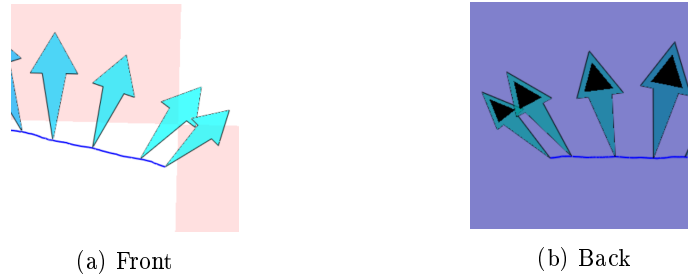


Fig. 4: Distinguishing the face of the arrow with a black triangle.

The three orientations of the arrow tip, surface, and left side of the surface represent the front, top, and left orientations of the body part in the initial T-stance pose, respectively. The arrow is generated as a polygon consisting of six vertices, as shown in Figure (4), and the standard values of its height  $h$  and width  $w$  are set to  $h = 0.12f$  and  $w = 0.08f$ , respectively. To distinguish between the front and back surfaces, a black triangle with standard height and width values of  $0.05f$  is marked on the back side, as shown in Figure 4(b). To

add time information, the color of the arrows is gradually changed from the beginning to the end of the visualization section based on the number of arrows generated. The target parts for arrow generation and the colors used are the same as those described in Section 4.1. To calculate the rotational speed  $r$ , our method uses Rodrigues' rotation formula to calculate the rotation angle  $\theta$  of a part in a frame. That is,

$$\theta = \frac{M_{00} + M_{11} + M_{22} - 1}{2} \quad (3)$$

where  $M$  is a  $3 \times 3$  rotation matrix representing the rotation between frames, which is computed using forward kinematics. Then,  $r$  is calculated by dividing  $\theta$  by the time interval between frames of motion. Because the amount of change in the rotational speed varies significantly among parts, it is necessary to adjust the size of the arrows. Therefore, our method normalizes the arrow size  $s_i$  by using the minimum arrow size  $s_{min}$  and larger of the maximum values of the rotational speeds of the part in the two input motions,  $r_{max}$ , as follows:

$$s_i = s_{min} + \frac{r_i}{r_{max}} s_{min}. \quad (4)$$

## 5.2 Adjusting the Drawing Interval

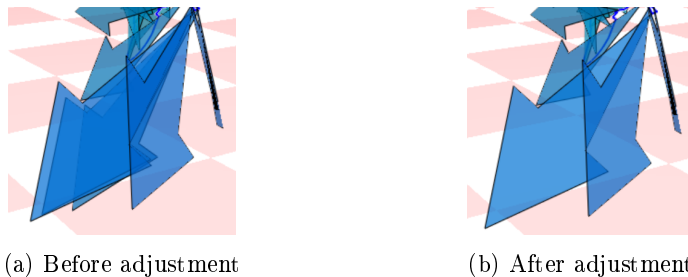


Fig. 5: The result of adjusting the number of arrows drawn depending on the viewpoint.

If the drawing interval is too narrow or wide, the visibility will be poor. Therefore, our method solves these problems by drawing arrows when the amount of rotation meets the threshold value  $t_r$ . When the range does not meet the threshold value, the arrows are drawn when the distance traveled meets the threshold value  $t_v$ . The amount of rotation  $t_r$  is the sum of the rotation angles for several frames, and the arrows indicate  $t_r = 0.45f$  and  $t_v = 0.3f$ .

In addition, as shown in Figure 5(a), if multiple arrows in the same direction overlap in succession, the visibility will deteriorate. Therefore, in this method, the distance between arrows is adjusted according to the viewpoint, as shown

in Figure 5(b). To achieve this, we define the intersection of the lines connecting both ends of the arrow as the representative point of the arrow. Then, if the distance between the representative points of adjacent arrows in the screen coordinate system is less than the threshold  $t_d$  and the angle between the two arrows is the threshold  $\theta_t$ , the arrow with larger distance between the origin point of the arrow and the camera in the world coordinate system is removed. In this study, we set  $t_d = 20.0f$  and  $\theta_t = \frac{\pi}{18}$ .

## 6 Experimental Results

### 6.1 Feature Grasping and Comparisons

We conducted experiments to evaluate the usefulness of this technique for grasping the motions of body parts. We confirmed whether the user could grasp changes in the features of body parts in a motion from spatial volumes and arrows, and whether the user could grasp the differences between two motions by comparing them. We applied our method to tennis shot forms of beginners and experts. We also applied our method to the batting motion of an expert baseball player and conducted an experiment to determine whether complex rotations could be understood from the state of the arrows. For these experiments, we prepared the motions of a beginner with a similar physique to that of an expert. The motion interval was from takeback to follow-through. The motions of a tennis forehand shot were captured using an optical motion capture system [9], and the motions of baseball batting were captured using an inertial motion capture system [10].

We present the results of generating volumes that visualize changes in the position and movement speed of the right hand during tennis forehand shots by an expert and a beginner. We also present the results of generating arrows that visualize the changes in the 3D orientation and rotational speed of the waist and chest in the same forehand shot motions, and the right hand in baseball batting. In addition, the postures at the moment of motion impact are shown in these visualization results.

**Visualization Results for Tennis Forehand Shots** As shown in Figure 6(a), the radius of the volume of the expert motion increased rapidly directly before impact, whereas the radius of the beginner motion in Figure 6(c) changed slowly throughout the motion. This is also observed in the shapes of the graphs in Figures 6(b) and 6(d). We also observe that the height of the starting point of the volume was lower than that of the expert. From these, we can infer that the beginner did not swing the racket strongly directly before the moment of impact, and the position of the right hand at takeback was low. Based on this, beginners can modify their motion by swinging the racket harder directly before impact and raising their right hand higher at takeback.

Observing the size of the arrows at the waist in Figures 7(a) and 7(c) reveals no significant difference overall, with both motions rapidly increasing directly

prior to impact. However, it can be observed from Figures 8(a) and 8(c) that the sizes of the arrows of the beginner’s motion decreased around impact, whereas those of the expert remained large. This can also be observed in Figures 7(b), 7(d), 8(b), and 8(d), which show the changes in the rotational speed at each site. In addition, while the orientation of the two parts was almost the same in the expert’s motion, the chest was facing more to the left than the waist in that of the beginner. Furthermore, it can be observed from Figures 8(a) and 8(c) that the orientations of the chest arrow at the beginning and end of the visualization section were more to the left in the beginner’s motion than in the expert’s one. From the above, it can be observed that there were problems in the beginner’s motion: the chest rotation speed decreased directly before impact, the upper body twist at takeback was small, and the upper body twisted back too much at the moment of impact and follow-through. Based on the information obtained, beginners can modify their own motion by being aware of a greater body twist at takeback and directly before impact, not slowing down their chest rotational speed, and not twisting the body back too far. In this connection, no changes in the direction of the chest or waist were observed, other than toward the front, in either motion.

The same information can be observed from Figures (6), (7), and (8), which show the results of similar visualizations for different movements of the same people. In addition, the visualization results from the other motions show changes in the feature values and differences between motions. According to these results, this approach is effective as a practice method for beginners to imitate the motions of experts.

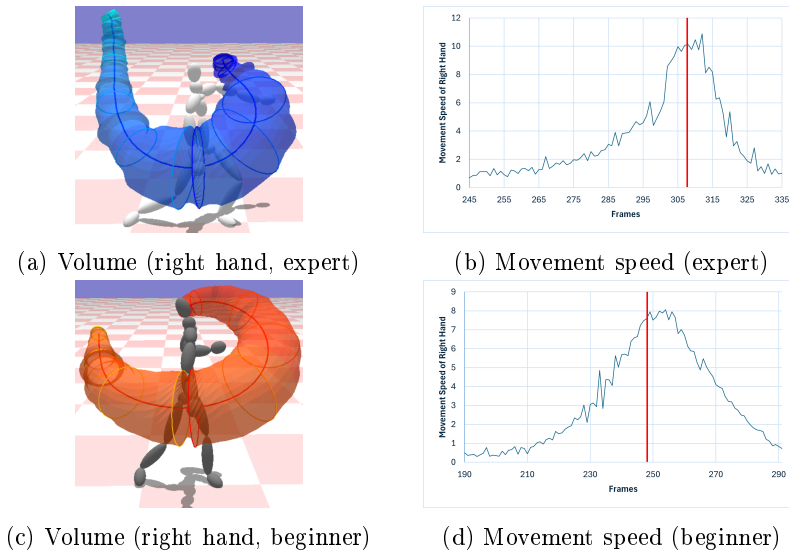
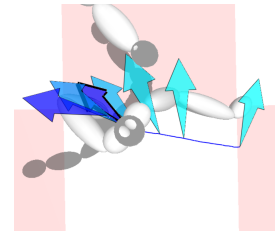
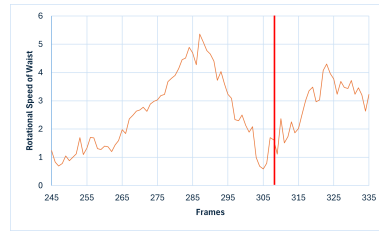


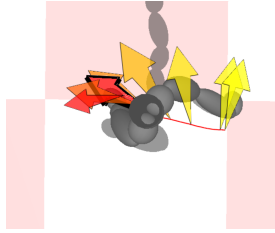
Fig. 6: Visualization results of changes in the movement speed of the right hand. The posture and red line in the graph are for the moment of impact.



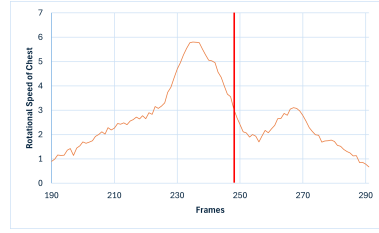
(a) Arrow (waist, expert)



(b) Rotational speed (expert)

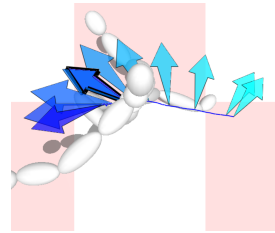


(c) Arrow (waist, beginner)

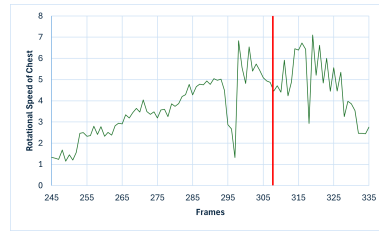


(d) Rotational speed (beginner)

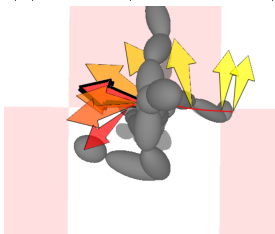
Fig. 7: Visualization results of changes in waist orientation and rotational speed. The arrows with thick outer frames and red line in the graph are for the moment of impact.



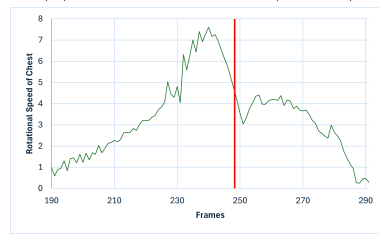
(a) Arrow (chest, expert)



(b) Rotational speed (expert)



(c) Arrow (chest, beginner)



(d) Rotational speed (beginner)

Fig. 8: Visualization results of changes in chest orientation and rotational speed. The arrows with thick outer frames and red line in the graph are for the moment of impact.

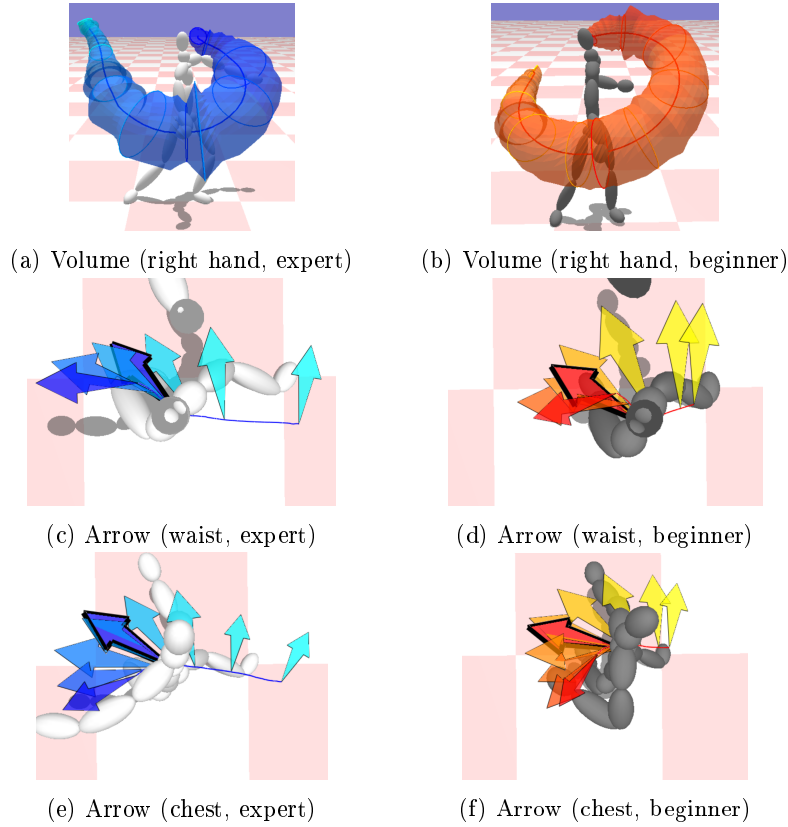


Fig. 9: Comparison of visualization results for different movements of the same people.

**Visualization Results for Baseball Batting** To confirm whether the method is also effective for movements with complex orientation changes, we applied it to the right hand, which rotates in a twisting direction during the baseball batting motion of a skilled baseball player. To confirm this, the visualization section was changed to from the point at which the twisting rotation began to the moment of impact, which was the endpoint. To improve the visibility, a stick figure representing the posture is not displayed. Note that the tip of the arrow represents the direction from the center of the palm towards the thumb; that is, the direction of the tip of the bat, and the surface represents the palm direction.

It can be observed from Figures 10(a) and 10(b) that this movement began to rotate in a twisting direction directly before the moment of impact and the direction of the tip of the arrow changed from vertically upwards to counter-clockwise when viewed from both the side of the hitting point and the side of the ball’s traveling direction. From this, we can infer that the expert rotated the bat, which was pointing vertically upwards from the expert’s perspective,

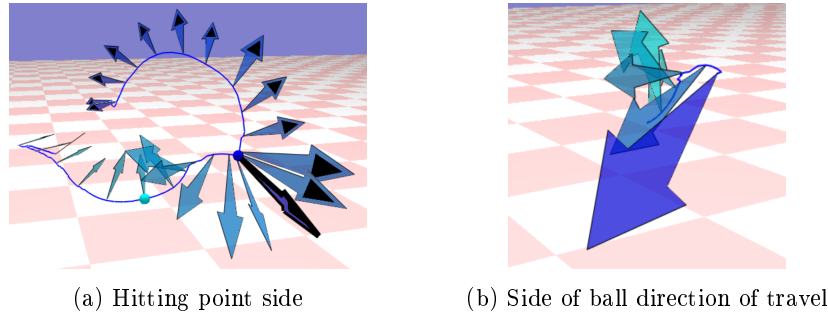


Fig. 10: Arrow generation results for rotation in the twisting direction. (a) The cyan sphere indicates the start of the visualization section, and the blue sphere indicates the end.

clockwise around the grip end of bat directly before impact, rotating it into a position where it could meet the hitting point. This confirms that our method can possibly be used to understand torsional rotations. However, the number of motions obtained was small; therefore, it could not be sufficiently validated. Thus, it is necessary to apply this method to a larger number of motions and confirm its usefulness for complex rotations such as torsional rotation.

## 6.2 Discussion

In this section, we explain the problems associated with our methods and discuss future challenges. First, when these methods are applied to body parts that move back and forth within the same range, the volumes and arrows overlap, resulting in poor visibility. To solve this problem, our system makes it possible to change the visualization section; however, if there are many back and forth movements, it is necessary to change the section finely and visualize it, which is time consuming. As such, a future challenge will be to make it possible to handle the movements of body parts that move back and forth in the same range.

In addition, our method smoothed the position and movement speed to make the surface of the volume smooth, but its shape remained bumpy. Consequently, it may be difficult to grasp how the features change. To generate the surface, we used a simple method of generating triangular polygons by specifying vertices. However, if the vertices are not properly specified, the shape of the volume will become distorted. Therefore, it is necessary to apply more effective smoothing and surface generation methods.

Furthermore, users may overlook these differences when comparing the volumes and arrows generated for each input action. Hence, it may be necessary to devise a method to visualize the differences in the changes in features and make them easier for users to understand.

## 7 Conclusion

We have proposed a method for visualizing changes in the features of body parts using the spatial volume and flat arrows. Our method simultaneously visualizes the changes in the position and movement speed of a body part by generating a volume along the trajectory of the body part, the radius of which changes according to the movement speed. In addition, we simultaneously visualize changes in the 3D orientation and rotational speed of the body part by generating flat arrows, the size of which changes according to the rotational speed. Our method can help users to understand how to move body parts and the differences between their own and expert motions. In the future, we plan to expand these methods by supporting parts that move back and forth within the same range, improving the smoothing process and surface generation method when generating the volume, and improving the visualization method.

## References

1. J. C. Chan, H. Leung, J. K. Tang, and T. Komura: A virtual reality dance training system using motion capture technology. *IEEE Transactions on Learning Technologies*, vol. 4, no. 2, pp. 187–195 (2011).
2. F. Anderson, T. Grossman, J. Matejka, and G. Fitzmaurice: YouMove: enhancing movement training with an augmented reality mirror. In *Proceedings of the 26th Annual ACM Symposium on User Interface Software and Technology*. ACM, pp. 311–320 (2013).
3. M. Kyan, G. Sun, H. Li, L. Zhong, P. Muneesawang, N. Dong, B. Elder, and L. Guan: An approach to ballet dance training through MS Kinect and visualization in a cave virtual reality environment. *ACM Transactions on Intelligent Systems and Technology (TIST)*, vol. 6, no. 2, Article No. 23 (2015).
4. J. E. Cutting: Representing motion in a static image: constraints and parallels in art, science, and popular culture. *Perception*, pp. 1165–1193 (2002).
5. H. Yasuda, R. Kaihara, S. Saito, and M. Nakajima: Motion Belts: Visualization of Human Motion Data on a Timeline. *IEICE Transactions on Information and Systems*, vol. E91.D, no. 4, pp. 1159–1167 (2008).
6. X. Zhang, T. Dekel, T. Xue, A. Owens, Q. He, J. Wu, S. Mueller, and W. T. Freeman: MoSculp: Interactive visualization of shape and time. In *Proceedings of the 31st Annual ACM Symposium on User Interface Software and Technology*, pp. 275–285 (2018).
7. M. Oshita: Motion Volume: Visualization of Human Motion Manifolds. In *17th ACM SIGGRAPH International Conference on Virtual-Reality Continuum and its Applications in Industry (VRCAI 2019)*, Article No. 7, pp. 1–7 (2019).
8. W. E. Lorensen and H. E. Cline: Marching cubes: A high resolution 3D surface construction algorithm. *Computer Graphics*, vol. 21, pp. 163–169 (1987).
9. Natural Point: Optitrack motive, <http://www.naturalpoint.com/>, last accessed 2024/09/11.
10. Perception Neuron: Neuron Studio, <https://neuronmocap.com/>, last accessed 2024/09/11.